Effect of the Antenna-Human Body Distance on the Antenna Matching in UWB WBAN Applications

Tommi Tuovinen, Timo Kumpuniemi, Kamya Yekeh Yazdandoost, Matti Hämäläinen, Jari Iinatti

Centre for Wireless Communications
University of Oulu
Oulu, Finland
{forename.surname}@ee.oulu.fi

***Abstract*—In this paper, the interaction between the ultra wideband (UWB) antenna and human body is considered and demonstrated in the range of 0 – 30 mm above the body surface, which could be practical operation distance for the on-body antenna. Two different planar UWB antennas (loop and dipole) are used for the examinations. First, the antenna performance in free space (FS) is shown. Then, the effect of the antenna-body distance on the antenna operation is analysed in the terms of the matching, i.e., reflection coefficient S_{11}. Measurements are carried out in the proximity of a real human body while the simulations are run by using the whole body model having a frequency-dependent behaviour. Observations are concluded to commensurate with the antenna field regions and the size of antenna's reactive near-field was satisfied to be an important factor in the evaluation of an acceptable on-body operation. No significant differences between different antennas were observed through investigations. Both antennas perform satisfactory when the distance is high enough. The results of this study are helpful to engineers and designers evaluating antennas for the use in UWB wireless body area network (WBAN) applications.**

Keywords—antenna-body interaction; reactive near-field region; ultra wideband (UWB) antenna

I. INTRODUCTION

Ultra wideband (UWB) wireless body area network (WBAN) systems have been a point of discussion in recent years. An international standard IEEE 802.15.6 [1] for a short-range, low power and highly reliable wireless communications was published in the first quarter of 2012 where UWB technology is defined as one physical (PHY) layer approach. The IEEE 802.15.6 standard is targeted to be used in the vicinity of human body or inside it. The first regulations for the UWB technology were announced in 2002 in the USA by the Federal Communication Commissions (FCC) [2], [3]. A vital role of the antenna to the entire system performance cannot be diminished in UWB WBAN applications. UWB antenna characteristics and their suitability for different applications are comprehensively discussed in [4]. A satisfactory on-body antenna 1) needs to be insensitive to the proximity of the body, and 2) it needs to have a radiation pattern that minimizes the link loss [5]. Moreover the body effect deteriorates the antenna performance also the tissues have a strong effect on the antenna operation. The IEEE 802.15.6 provides, recommends, and proposes to consider the antenna characteristics due to the presence of a person. There are number of studies in the open literature that present the antenna performance close to the body, e.g., [6]-[8]. Generally, these studies cover the antenna performance and operation analysis only when it is positioned (usually) on contact with the tissues or at some specific distances D (e.g., D = 0, 5, or 10 mm) from the body.

This paper examines and analyses the effect of the UWB antenna-human body operating distance D on the antenna operation through $0 \leq D \leq 30$ mm in steps of 2 mm with two different antennas. The aim of this study is to evaluate, demonstrate and consider the antenna matching at different distances in the close proximity of the real human body by measurements and additionally by simulations. The simulations use a whole body model, which is adjusted to utilize a frequency-dependent behaviour for the UWB frequencies. Simulations are done with computer simulation technology (CST) microwave studio (MWS) [9] using finite integration technique (FIT). This study is the continuation of investigations presented in [10]-[12].

II. MEASUREMENT AND SIMULATION SETUP

A. Two Planar UWB Antennas

Planar UWB antennas used in the examinations are shown in Fig. 1: a) dipole and b) double (slot) loop. The dipole structure is first published in [10] and also used in the investigations in [12]. The loop structure can be found the first time in [13] and utilized further in [14]. In this paper, an alternative substrate material is experimented as it is changed from FR4 (Glass Reinforced Epoxy) to TRF-43 (polytetrafluoroethylene, PTFE-based) [15] substrate. The updated substrate TRF-43 has some attractive features for actual on-body scenarios that might cause issues with FR4: for instance, a better loss tangent $tan\delta$ than FR4 ($tan\delta$ = 0.025 for FR4 and $tan\delta$ = 0.0035 for TRF-43 @ 10 GHz) but also lower moisture absorption compared with FR4 (roughly tenfold lower) which might be a problem, e.g., in an outdoor usage and for the on-body usage, for instance, when the body perspires. Especially, the moisture absorption might cause issues, since the matching for UWB antennas is very sensitive for little changes in the antenna pattern (i.e., in the shape of the radiator). However, FR4 is clearly cheaper and a good free space (FS) performance can be also achieved with it. Due to the trial of TRF-43 both antennas are slightly reshaped and different UWB antenna parameters optimized for the new substrate material. TRF-43 achieves a corresponding dielectric constant of ε_r = 4.3 (+/- 0.15) as FR4. For the simulations, a 6-point loss tangent of $tan\delta$ = 0.0027 @ 1 GHz, 0.0028 @ 3 GHz and 5 GHz, 0.0029 @ 7 GHz, 0.0031 @ 9 GHz, and 0.0035 @ 10 GHz [15] was applied.

978-1-4673-5772-2/13/$31.00 ©2013 IEEE

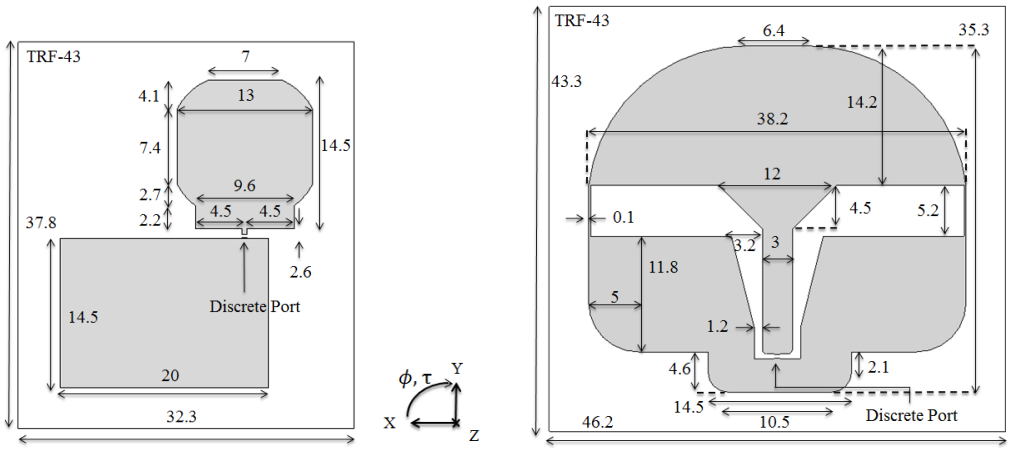

Figure 1. The CST simulation models of the planar UWB antennas in the investigations: a) (asymmetric) dipole and b) double (slot) loop antenna. Dimensions are in mm. The 18 µm-thick (i.e., the copper cladding thickness) antenna radiators are on the top side of the 1.63 mm-thick (i.e., the dielectric thickness) TRF-43 substrate in the direction of z axis.

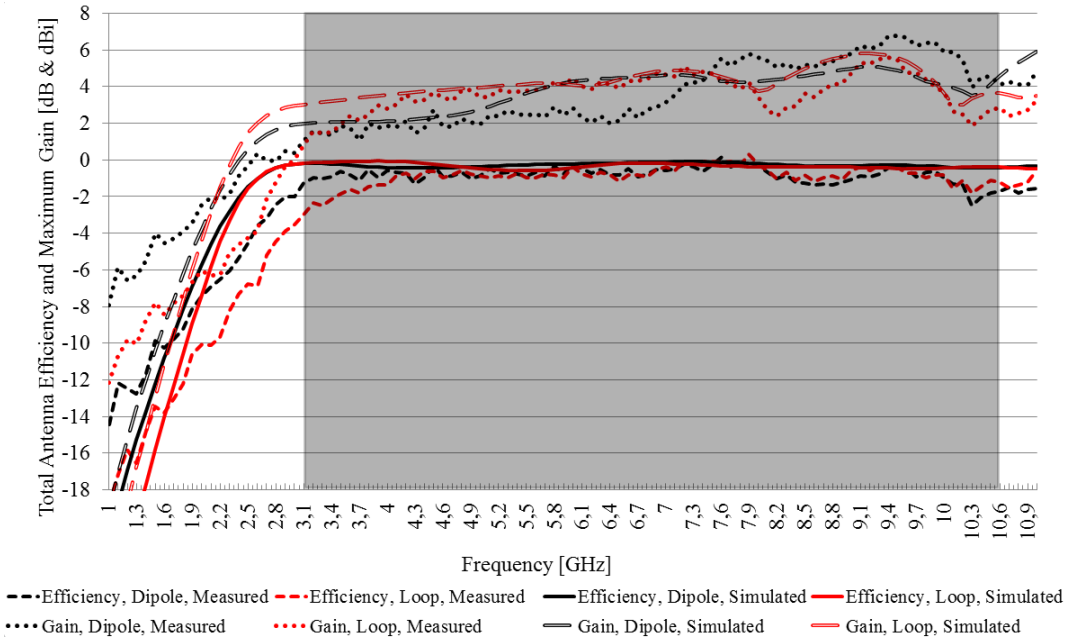

Figure 2. The measured and simulated total antenna efficiency e_0 [dB] and realized maximum gain [dBi]. Grey area is the FCC UWB band of 3.1 – 10.6 GHz.

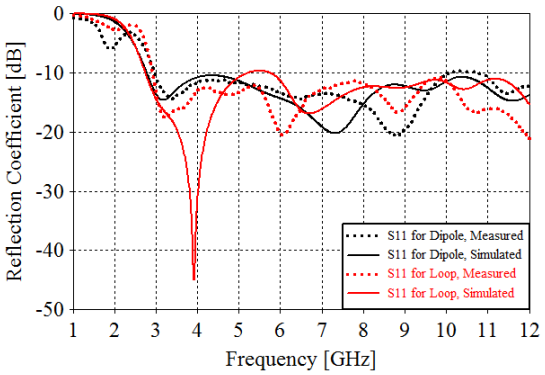

Figure 3. The measured and simulated reflection coefficient S_{11} [dB] in the free space.

The prototypes of each antenna were manufactured and their FS performances were first measured with a Satimo Starlab [16] chamber (valid from 800 MHz to 18 GHz). Fig. 2 collects the data of the measured and simulated total antenna efficiency and realized maximum gain for the presented antennas while the reflection coefficients S_{11} are presented in Fig. 3. Both antennas show an appealing FS operation. Although the simulated and measured S_{11} values are very similar, the small difference can be explained due to the difference of cabling (a semi-rigid cable in measurements) and feeding (a discrete port in simulations).

B. Measurement Setup

Fig. 4 demonstrates the measurement setup for the antenna under test (AUT) S_{11} measurements in the vicinity of the person under test, i.e., the first author of this paper. S_{11} values were measured for the frequencies of 1 – 12 GHz (the bandwidth of 11 GHz) by using an Agilent 8720ES vector network analyser (VNA) [17]. The VNA was controlled with a laptop computer using LabVIEW software through the general purpose interface bus (GPIB) of the VNA. When the

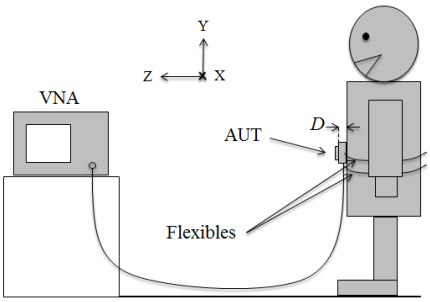

Figure 4. The measurement setup in an anechoic chamber. The antenna and test person have the same coordinates as determined in the figure.

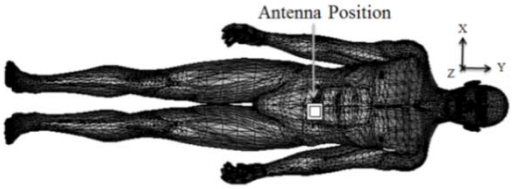

Figure 5. The simulation setup for CST MWS. The antenna and whole human body model have the same coordinates as determined in the figure.

test person was standing still in the chamber, 20 sweeps across the measurement bandwidth were recorded. The results shown in the figures 6a)-h) are the averages of the absolute values of the measured data. The measurement time to record 20 sweeps in a static situation was approximately 70 sec where the time for one individual sweep consisted of a 800 ms sweep time of the VNA added with the necessary processing time to save the data. The number of points over the band was 1601. The AUT was placed on the abdomen of the person at the position shown in Fig. 4. The height of the test person was 183 cm and the AUT-ground distance was 110 cm. The gap, i.e., the operation distance D between the antenna and the body was filled with a material called Rohacell 31 HF (RC 31 HF) [18], which has electrical properties close to air (ε_r = 1.046 @ 10 GHz). The blocks of RC 31 HF with thicknesses of 0 mm ≤ D ≤ 30 mm at steps of 2 mm were positioned between the AUT and the person in order to verify the exact antenna distance. The radiation characteristics and S_{11}s were also measured in the FS conditions with a block of RC 31 HF in order to verify the electrical invisibility of the material from the antenna's perspective. Two flexible ribbons were used to keep the antenna in the right position. The test person had a cotton T-shirt on the upper body having the thickness of roughly 1 mm.

C. Simulation Setup

Simulations were performed for distances of 0 ≤ D ≤ 30 mm in steps of 1 mm with the CST's whole human body model. The body model is presented in Fig. 5 and made of dispersive skin according to (1), as the electrical dispersion of the model for UWB frequencies is determined by the 2nd order Debye model in this study [19], [20]

$$\varepsilon = \varepsilon' - j\varepsilon'' = \varepsilon_\infty + \frac{\varepsilon_{s1}-\varepsilon_\infty}{1+j\omega\tau_1} + \frac{\varepsilon_{s2}-\varepsilon_\infty}{1+j\omega\tau_2}, \quad (1)$$

where ε' and ε'' are real and imaginary part of permittivity, ω is angular frequency (= $2\pi f$), ε_∞ is the dielectric constant at the higher frequency limit epsilon (infinity) value, ε_s is the value at lower frequency limit epsilon (static) value, and τ is relaxation time. The values of the dispersion model for the body model are defined according to [19], [20] and the online database [21]. The used values can be found, e.g., in [10]-[12]. In the simulations, the blocks of RC 31 HF were modelled to have a 4-point loss tangent of $tan\delta$ = 0.0002 @ 2.5 GHz, 0.0016 @ 5 GHz, 0.0017 @ 10 GHz and 0.0106 @ 26.5 GHz based on the values in the data sheet [18].

III. Results

This section presents the results of different antenna-body distances in terms of S_{11}. The main aim here is to demonstrate how the matching behaviour changes in the close proximity of the body. Based on the observed results in measurements, some significant distances are presented here for each antenna, and also for simulations, respectively.

Figs. 6a)-h) show the measurement results for the real human body and the simulation results for the whole body model. The FS matching is plotted as a reference for the body results to the figures where the higher distances are presented. When analysing the dipole and loop antennas the matching is observed to have the widest bandwidth (based on lower and higher – 10 dB band edges) at D = 0 mm. In this case, the antenna performance is however the poorest, since a significant amount of the power is dissipated to the tissues, as demonstrated with figures in [10], [11]. It can be attained that the S_{11} starts to vary strongly during the first millimetres, especially for the loop antenna where the frequencies for resonances vary strongly as a function of D. It is observed that neither of antennas covers the entire FCC – 10 dB UWB band after the distance is increased for first millimetres. The poorest matching for both antennas in the measurements is attained at D = 2 mm. It should be also taken into account that the presented distances are measured from the bottom of the substrate to the skin surface hence the practical coppering-body distance is 1.63 mm higher than the presented values. The antenna matchings' start to widen slowly after the poorest matching is achieved. The matching widens until it reaches a behaviour close to the result of FS, which is found around D = 18 - 20 mm for both antennas based on the S_{11} results. After the observed range of D = 18 – 20 mm, the operation stay notable stable.

As a general observation it can be mentioned that the matching in higher frequencies of UWB band stays rather stable after the distances of first millimetres is exceeded. The most significant changes and variations in the distances of 0 – 20 mm are observed mainly in lower frequencies. In order to explain this behaviour, knowledge of the antenna field regions is required: the closest space surrounding an antenna, i.e., its near-field (N-F) is subdivided into a reactive ($R < R_1$) and a radiating N-F ($R_1 < R < R_2$) [22]. R_1 is defined based on the largest dimension of the antenna D_L and wavelength λ as [22]

$$R_1 = 0.62\sqrt{D_L^3/\lambda}. \quad (2)$$

For the electrically small antenna (ESA), the radius of the Wheeler's radiansphere can be defined as [24]

$$R_W = \frac{\lambda}{2\pi}. \quad (3)$$

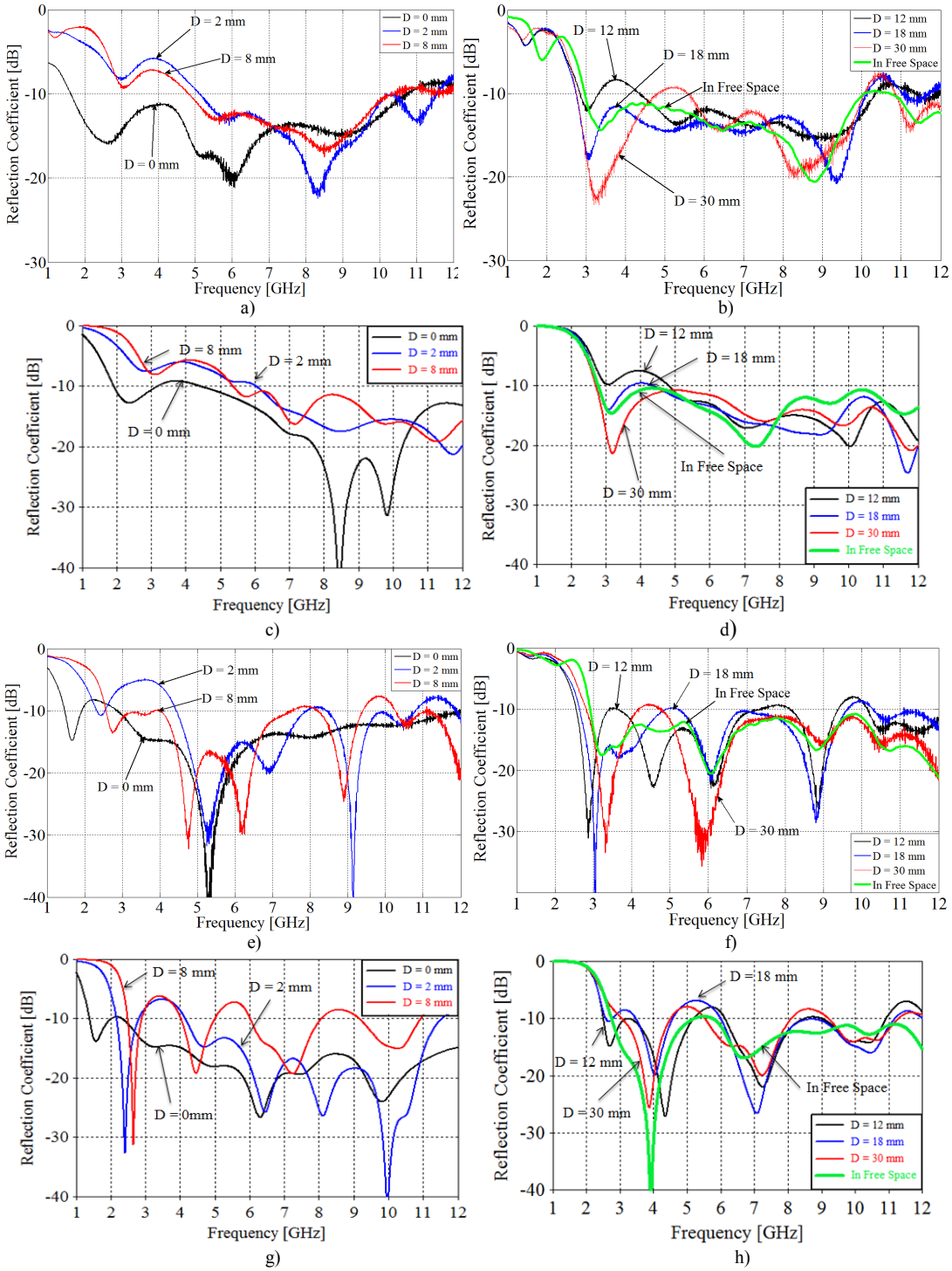

Figure 6. The antenna-human body distances in terms the reflection coefficient S_{11}: a)-b) measurements for the dipole, c)-d) simulations for the dipole, e)-f) measurements for the loop, and g)-h) simulations for the loop. The presented distance is measured from the middle point of the bottom of TRF-43 substrate to the top of the skin. The measurement results are processed with Matlab and the simulation results with the CST.

It is intelligible that the UWB antenna cannot be ESA, at least over the entire band (3.1 – 10.6 GHz) as explained, e.g., in [25]. An individual antenna analysis, e.g., for the loop based on the impedance behaviour or radiation patterns, proves it to work in a different way than corresponding ESA loop. However in the proximity of body, that antenna seems to work as ESA. It is noted, the utilized UWB antennas are electrically large antennas for most of the frequency range and those can be considered to be partially ESA. Furthermore, as the comparison between the presented boundary definitions in (2)-(3) and the results received here is performed (see Table I), (3) really seems to work better for UWB antenna behaviour close to the body when explaining the results. For further discussion, the energy stored into the antenna in the reactive N-F region, is significantly higher compared with its radiated energy. When the body tissues appear in the area of reactive N-F, there will

TABLE I. WAVELENGTH AND BOUNDARY DISTANCES OF REACTIVE NEAR-FIELD REGIONS AT DIFFERENT FREQUENCIES

Parameters	Dipole				Double Loop			
	Frequency [GHz]				*Frequency* [GHz]			
	3	5	7	10	3	5	7	10
Wavelength λ [mm]	96.0	57.6	41.1	28.8	96.0	57.6	41.1	28.8
Largest dimension D_L [mm]	37.1				40.9			
Reactive near-field R_1 [mm]	14.3	18.5	21.9	26.1	16.6	21.4	25.3	30.2
Wheeler's radiansphere R_w [mm]	15.3	9.17	6.5	4.6	15.3	9.17	6.5	4.6

be changes on the permittivity value of the area close to the antenna structure hence causing significant changes in its operation. In the radiating N-F, the proportion of the energy stored in an antenna is minor compared with the field strength. As the operating distance increases, the reactive N-F decreases.

IV. CONCLUSIONS

The effect of the antenna-body operation distance for the matching results was considered and demonstrated by measurements and simulations in this paper. Two planar UWB antennas were used for the examinations. Strong variations on the reflection coefficient S_{11} were observed among the investigated distances for both antennas. Significant differences between antennas were not observed: both of them operate well when the distance is high enough. The size of the antennas' reactive near-field based on the Wheeler's radiansphere was concluded to be the important factor in the evaluation of the shortest UWB antenna-human body operating distance.

V. ACKNOWLEDGEMENTS

This work is funded by the Finnish Funding Agency for Technology and Innovation (Tekes) through two research projects: Enabling future Wireless Healthcare Systems (EWiHS) and Wireless Body Area Network for Health and Medical Care (WiBAN-HAM). Tauno Tönning, Emil Aaltonen, TES and HPY foundations are also acknowledged. Dr. Erkki Salonen and Dr. Markus Berg are acknowledged for fruitful discussions related to the antenna field theory.

REFERENCES

[1] IEEE Standard for Local and Metropolitan Area Networks, IEEE 802.15.6-2012 – Part 15.6: Wireless Body Area networks, 2012.

[2] First Report and Order in the matter of revision of Part 15 of the Commission's rules regarding ultrawideband transmission systems, Federal Communications Commission, ET-Docket 98-153, FCC 02-48, 2002.

[3] I. Oppermann, M. Hämäläinen, and J. Iinatti, UWB Theory and Application. England: John Wiley & Sons, 2004, pp. 1-7 and 129-156.

[4] G. Adamiuk, T. Zwick, and W. Wiesbeck, "UWB antennas for communication systems," Proc of IEEE, vol. 100, no. 7, pp. 2308-2321, July 2012.

[5] P. S. Hall, and Y. Hao, Antennas and Propagation for Body-Centric Wireless Communications. Norwood: Artech House, 2012, 2nd ed., pp. 1-16 and 139-160.

[6] T. S. P. See, and Z. N. Chen, "Experimental characterization of UWB antennas for on-body communications," IEEE Trans. Antennas Propag., vol. 57, no. 4, pp. 866-874, April 2004.

[7] Z. N. Chen, A. Cai, T. S. P. See, X. Qing, and M. Y. W. Chia, "Small planar UWB antennas in proximity of the human head," IEEE Trans. Microw. Theory Tech., vol. 54, vo. 4, pp. 1846-1857, April 2006.

[8] N. Chahat, M. Zhadobov, R. Sauleau, and K. Ito, "A compact UWB antenna for on-body applications," IEEE Trans. Antennas Propag., vol. 59, vo. 4, pp. 1123-1131, April 2011.

[9] CST Microwave Studio [Online]. Available: http://www.cst.com.

[10] T. Tuovinen, M. Berg, K. Yekeh Yazdandoost, E. Salonen, and J. Iinatti, "Reactive near-field region radiation of planar UWB antennas close to a dispersive tissue model," in Proc. 8th Int. Loughborough. Ant. Propag. Conf. (LAPC), Nov. 2012, United Kingdom, pp. 1-4

[11] T. Tuovinen, M. Berg, K. Yekeh Yazdandoost, E. Salonen, and J. Iinatti, "Radiation properties of the planar UWB dipole antenna in the proximity of dispersive body models," in Proc. 7th Int. Conf. on BANs (BodyNets), Sep. 2012, Oslo, Norway, pp. 1-7.

[12] T. Tuovinen, M. Berg, K. Yekeh Yazdandoost, E. Salonen, and J. Iinatti, "Impedance behaviour of planar UWB antennas in the vicinity of a dispersive tissue model," in Proc. 8th Int. Loughborough. Ant. Propag. Conf. (LAPC), Nov. 2012, United Kingdom, pp. 1-4.

[13] T. Tuovinen, K. Yekeh Yazdandoost, and J. Iinatti, "Comparison of the performance of the two different UWB antennas for the use in WBAN on-body communications," in Proc. 6th Europ. Conf. Antennas Propagat. (EuCAP), March 2012, Prague, Czech, pp. 3371-3374.

[14] M. Särestöniemi, T. Tuovinen, M. Hämäläinen, K. Yekeh Yazdandoost, and J. Iinatti, "Channel modeling for UWB WBAN on-off body communication link with integration technique," in Proc. 7th Int. Conf. on BANs (BodyNets), Sep. 2012, Oslo, Norway, pp. 1-7.

[15] Taconic (accessed on October 2012), TRF -41, -43, -45: Low-loss ceramic-filled PTFE [Online]. Available: http://www.taconic-add.com/pdf/trf.pdf.

[16] Satimo Starlab (accessed on October 2012), [Online]. Available: http://www.satimo.com/content/products/starlab.

[17] Agilent (accessed on October 2012), [Online]. Available: http://www.home.agilent.com/agilent/home.jspx?cc=FI&lc=fin.

[18] Rohacell (accessed on October 2012), [Online]. Available: http://www.rohacell.com/sites/dc/Downloadcenter/Evonik/Product/ROHACELL/product-information/ROHACELL%20HF%20Product%20Information.pdf.

[19] F.S. Barnes, and B. Greenebaum, Bioengineering and Biophysical Aspects of Electromagnetic Fields. Boca Raton: Taylor & Francis Group, 2007, pp.58-59, 316-317, 340-343.

[20] O.P. Gandhi, B.Q. Gao, and J.Y. Chen, "A frequency-dependent finite-difference time-domain formulation for general dispersive media," IEEE Trans. Antennas Propag., vol. 41, no. 4, pp. 658-665, April 1993.

[21] Calculation of the Dielectric Properties of Body Tissues in the frequency range 10 Hz – 100 GHz, (accessed on October 2012), [Online]. Available: http://niremf.ifac.cnr.it/tissprop/htmlclie/htmlclie.htm.

[22] C. A. Balanis, Antenna Theory Analysis and Design. Canada: John Wiley & Sons, 3rd ed., 2005, pp. 27-68.

[23] A. V. Räisänen, and A. Lehto, Radio Engineering for Wireless Communication and Sensor Applications. Norwood: Artech House, 2003, pp. 205-209.

[24] H. A. Wheeler, "The radiansphere around a small antenna," in Proc. of the Inst. Radio Eng. (IRE), 1959, pp. 1325-1331.

[25] R. C. Hansen, Electrically Small, Superdirective and Superconducting Antennas. John Wiley & Sons, 2006, pp. 10-48.